

Minimum reinforcement and ductility index of lightly reinforced concrete beams

Alessandro P. Fantilli^{*}, Bernardino Chiaia^a and Andrea Gorino^b

*Department of Structural, Building and Geotechnical Engineering, Politecnico di Torino,
Corso Duca degli Abruzzi 24, 10129 Torino, Italy*

(Received July 13, 2016, Revised September 10, 2016, Accepted September 11, 2016)

Abstract. Nonlinear models, capable of taking into account all the phenomena involved in the cracking and in the failure of lightly reinforced concrete beams, are nowadays available for a rigorous calculation of the minimum reinforcement. To simplify the current approaches, a new procedure is proposed in this paper. Specifically, the ductility index, which is lower than zero for under-reinforced concrete beams in bending, is introduced. The results of a general model, as well as the data measured in several tests, reveal the existence of two linear relationships between ductility index, crack width, and the amount of steel reinforcement. The above relationships can be applied to a wide range of lightly reinforced concrete beams, regardless of the geometrical dimensions and of the mechanical properties of materials. Accordingly, if only a few tests are combined with this linear relationships, a new design-by-testing procedure can be used to calculate the minimum reinforcement, which guarantees both the control of cracking in service and the ductility at failure.

Keywords: lightly reinforced concrete beams; bending moment; minimum reinforcement; ultimate limit state; serviceability limit state; ductility index

1. Introduction

According to building code requirements (ACI 2014, Fib 2012), a minimum quantity of steel reinforcement needs to be provided in the tensile zones of concrete beams in bending (Levi 1985). In the serviceability state, a suitable amount of reinforcement prevents the growth of wide cracks and, consequently, the penetration of aggressive substances that compromise the durability of reinforced concrete structures. At the failure point, the minimum reinforcement area $A_{s,min}$ guarantees that cracking of concrete in tension occurs before the yielding of rebar, and avoids the brittle response of lightly reinforced concrete (LRC) beams. In this way, the ultimate bending moment M_u (herein assumed to be coincident with the yielding moment) is larger than the effective cracking moment M_{cr*} , corresponding to the peak of moment during the growth of the first crack. According to Maldague (1965), M_{cr*} is always larger than M_{cr} , defined as the first cracking moment at which the tensile strength of concrete is attained in the tension fiber of the cross-

^{*}Corresponding author, Associate Professor, E-mail: alessandro.fantilli@polito.it

^aProfessor, E-mail: bernardino.chiaia@polito.it

^bPh.D. Student, E-mail: andrea.gorino@polito.it

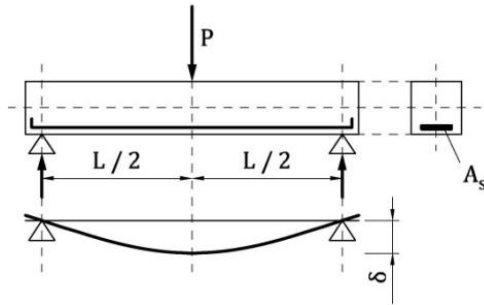


Fig. 1(a) Behavior of LRC beams (Ruiz, Elices *et al.* 1999): three point bending test

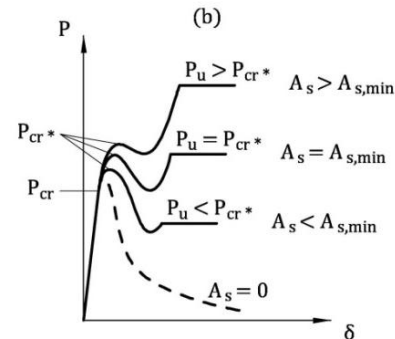


Fig. 1(b) Behavior of LRC beams (Ruiz, Elices *et al.* 1999): load - midspan deflection curves as a function of the cross-sectional area of rebar

section.

Similarly, the load applied to a three point bending beam has to satisfy the following condition (see Fig. (1))

$$P_u \geq P_{cr^*} \quad (1)$$

where P_u and P_{cr^*} are the loads that produce M_u and M_{cr^*} , respectively, in the midspan cross-section of the beam depicted in Fig. 1(a). Hence, when $M_u = M_{cr^*}$ (or $P_u = P_{cr^*}$) the minimum reinforcement for static reasons is correspondingly defined, independently of the midspan deflection δ of the beam (Fig. 1(b)). In other words, the ductility of LRC beams is defined by the strength, whereas the so-called plastic rotation measures the ductility of ordinary and over-reinforced concrete beams (CEB 1998). This concept is of paramount importance when massive concrete structures are realized (Rizk and Marzouk 2011).

For the theoretical evaluation of $A_{s,min}$, some nonlinear models must be applied, such as the bond-slip between rebar and concrete and the fracture mechanics of concrete in tension (Bažant and Cedolin 1991). The same mechanisms also influence the crack width and the crack spacing during the serviceability state (Fib 2000). Nevertheless, a univocally accepted approach, able to predict the crack pattern of reinforced concrete beams, does not exist despite the huge number of models available in the current literature (Borosnyói and Balázs 2005).

In the same way, a global and straightforward approach for the evaluation of $A_{s,min}$ was not provided by the numerical and experimental analyses performed in the past decades (Carpinteri 1999). For this reason, code rules suggest the use of simplified formulae for $A_{s,min}$, in order to satisfy both the serviceability and the ultimate limit states. To be more precise, the following symbolic formula, derived from reinforced concrete ties, is adapted by ACI 318-14 (ACI 2014) and Model Code 2010 (Fib 2012) to beams

$$A_{s,min} = \beta \cdot \frac{f_{ct}}{f_y} \cdot B \cdot d \quad (2)$$

Where β = coefficient depending on the model uncertainties, on the different state of stress between reinforced concrete beams and ties, and on the depth of the tensile zone: f_{ct} = tensile strength of concrete; f_y = yielding strength of steel rebar; B and d = width and effective depth,

respectively, of a beam cross-section. Similar formulae have also been proposed by other building codes and Authors (Seguirant, Brice *et al.* 2010).

Some geometrical aspects that affect $A_{s,min}$, such as the size effect produced by the beam depth (Carpinteri, Cadamuro *et al.* 2014) and by the bar diameter (Fantilli, Ferretti *et al.* 2005), are not taken into account by Eq. (2). As a result, the evaluation of the minimum reinforcement with Eq. (2) is only approximated. Hence, the aim of the present paper is to introduce a more effective approach to calculate $A_{s,min}$, which should be based on the real response of LRC beams. A new simple procedure, capable of predicting the brittle/ductile behavior of LRC beams and the minimum reinforcement, is proposed in the following. It is the result of both the theoretical and experimental investigations described in the next sections.

According to Fantilli, Ferretti *et al.* (1999), a block of LRC beam in three point bending, failing in the presence of a single flexural crack, is modelled. As shown in Fig. 2(a), the portion of the beam is delimited by the cracked cross-section (the midspan cross-section 0-0) and the so-

2. General model for LRC beams

2.1 Formulation of the problem

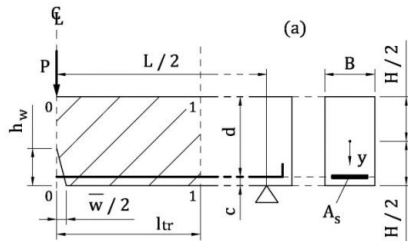


Fig. 2(a) General model for LRC beams in bending: A portion of the beam with a single crack

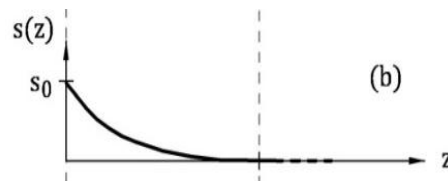


Fig. 2(b) General model for LRC beams in bending: Slips between rebar and concrete in tension

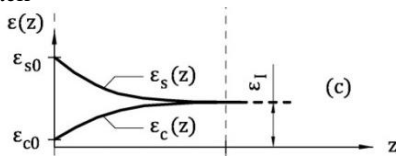


Fig. 2(c) General model for LRC beams in bending: Strains of rebar and concrete in tension

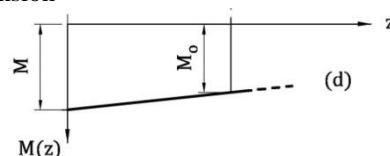


Fig. 2(d) General model for LRC beams in bending: Diagram of bending moment

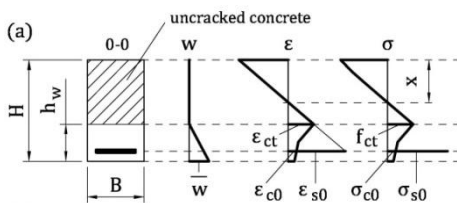


Fig. 3(a) Boundaries of the portion of the beam with a single crack: Stresses and strains in the cracked cross-section

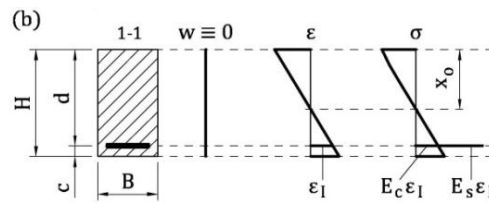


Fig. 3(b) Boundaries of the portion of the beam with a single crack: stresses and strains in the Stage I (or perfect bond) cross-section

called Stage I cross-section (cross-section 1-1), in which the perfect bond between steel and concrete is re-established. Within the block of length l_{tr} (= transfer length), as the horizontal coordinate z increases, stresses move from steel to concrete in tension, due to the bond-slip mechanism acting at the interface of the materials (Fig. 2). At the level of reinforcement, the slip s vanishes in the Stage I cross-section (Fig. 2(b)), where concrete strain ε_c equates steel strain ε_s (Fig. 2(c)). In the cross-section 0-0 (Fig. 3(a)), a linear strain profile along uncracked concrete and steel in tension is assumed. Conversely, in the cracked zone (of depth h_w) crack width w is supposed to linearly decrease from the bottom of the beam (where $w=\bar{w}$) to the crack tip (where $w=0$), in spite of the presence of the reinforcement. On the other hand, in the Stage I cross-section (Fig. 3(b)), the hypothesis of perfect bond makes the evaluation of steel and concrete strain ε_t , at the level of reinforcement, possible by means of the well-known linear elastic formula

$$\varepsilon_t = \varepsilon_s = \varepsilon_c = \frac{M_o}{E_o \cdot I_o} \cdot (d - x_o) \quad (3)$$

where M_o = bending moment in the Stage I cross-section; $E_o \cdot I_o$ = flexural rigidity of the composite cross-section; and x_o = distance from the top edge to the neutral axis in the composite cross-section. Within the transfer length, $M_o = M$ can be assumed (where M = bending moment in the cracked cross-section according to Fig. 2(d)). In such zone of the beam, the interaction between steel and concrete is described by the following equilibrium and compatibility equations

$$\frac{d\sigma_s}{dz} = -\frac{p_s}{A_s} \cdot \tau[s(z)] = -\frac{4}{\phi} \cdot \tau[s(z)] \quad (4)$$

$$\frac{ds}{dz} = -[\varepsilon_s(z) - \varepsilon_c(z)] \quad (5)$$

where σ_s = stress of steel rebar; p_s , A_s , and ϕ = perimeter, cross-sectional area, and nominal diameter of rebar, respectively; τ and s = bond stress and corresponding slip between steel and concrete.

In the absence of an external axial load ($N = 0$), the resultant of axial stresses becomes

$$N = \int_{A_c} \sigma_c dA + \sigma_s \cdot A_s = 0 \quad (6)$$

where σ_c = concrete stresses; A_c and A_s = cross-sectional areas of concrete and steel rebar, respectively.

Assuming y as the vertical coordinate (Fig. 2(a)), the internal bending moment M can be computed as follows

$$M = \int_{A_c} \sigma_c \cdot y dA + \sigma_s \cdot A_s \cdot \left(\frac{H}{2} - c \right) \quad (7)$$

where H = beam depth; and c = concrete cover (distance from the centroid of the rebar to the bottom edge of the cross-section).

In accordance with Fantilli and Chiaia (2013), steel strain decrements and concrete strain increments at the level of reinforcement are similar

$$\epsilon_s(z) = \epsilon_{s0} - \chi(z) \cdot (\epsilon_{s0} - \epsilon_1) \tag{8}$$

$$\epsilon_c(z) = \epsilon_{c0} - \chi(z) \cdot (\epsilon_{c0} - \epsilon_1) \tag{9}$$

where ϵ_{s0} and ϵ_{c0} = steel and concrete strains at level of reinforcement in the cracked cross-section; and χ = similarity coefficient. It should be remarked that the strain ϵ_{c0} can be obtained from the corresponding stress, by assuming the linear elastic behavior of uncracked concrete.

To solve Eqs. (4)-(9), the following boundary conditions are needed

$$s_0 = \frac{\bar{w}}{2} \cdot \frac{h_w - c}{h_w} \tag{10}$$

$$s(z = l_{tr}) = 0 \tag{11}$$

$$\epsilon_s(z = l_{tr}) = \epsilon_c(z = l_{tr}) \tag{12}$$

In Eq. (10), the slip s_0 in the cracked cross-section is equal to half of crack width at the level of reinforcement. Conversely, in the Stage I cross-section, Eq. (11) and Eq. (12) impose, respectively, the absence of slip and its stationary state. The latter condition is equivalent to consider the same strain in steel and concrete at level of reinforcement.

2.2 Material behavior

To model the stress-strain relationship σ_c - ϵ_c of concrete in compression, the ascending branch of the Sargin's parabola (Fib 2012) is used (Fig. 4(a))

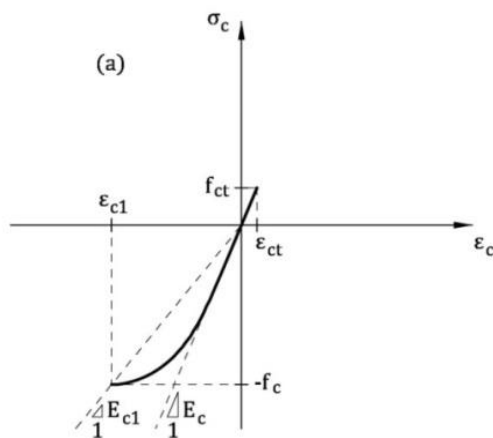


Fig. 4(a) Constitutive laws of materials (Fib 2012): Sargin's parabola for the concrete in compression, and linear elastic law for the uncracked concrete in tension

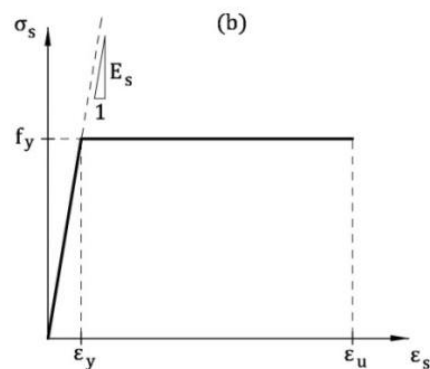


Fig. 4(b) Constitutive laws of materials (Fib 2012): Elastic-perfectly plastic law for steel rebar

$$\sigma_c = -f_c \cdot \left[\frac{k \cdot \eta - \eta^2}{1 + (k-2) \cdot \eta} \right] \text{ for } \varepsilon_{c1} < \varepsilon_c \leq 0 \quad (13)$$

where f_c = cylindrical compressive strength of concrete (mean value); $k = E_c/E_{c1}$ = plasticity number (i.e., the ratio between the tangent modulus of elasticity at the origin of the stress-strain diagram E_c , and the secant modulus from the origin to the peak of compressive stress E_{c1}); $\eta = \varepsilon_c/\varepsilon_{c1}$ = compressive strain normalized with respect to ε_{c1} (= strain at the peak of stress).

The following linear elastic constitutive law (Fig. 4(a)) is adopted for the uncracked concrete in tension

$$\sigma_c = E_c \cdot \varepsilon_c \text{ for } 0 < \varepsilon_c \leq \varepsilon_{ct} = f_{ct}/E_c \quad (14)$$

According to Model Code 2010 (Fib 2012), the mean tensile strength of concrete f_{ct} can be estimated from f_c (expressed in MPa)

$$f_{ct} = 0.3 \cdot (f_c - 8)^{2/3} \text{ for } f_c \leq 58 \text{ MPa} \quad (15a)$$

$$f_{ct} = 2.12 \cdot \ln(1 + 0.1 \cdot f_c) \text{ for } f_c > 58 \text{ MPa} \quad (15b)$$

After the linear elastic constitutive law in tension, the “fictitious crack model” is adopted to reproduce the behavior of cracked concrete. It consists on the following bilinear stress-crack opening displacement curve σ_c - w , also shown in Fig. 5(a) (Fib 2012)

$$\sigma_c = f_{ct} \cdot \left(1.0 - 0.8 \cdot \frac{w}{w_1} \right) \text{ for } 0 < w \leq w_1 \quad (16a)$$

$$\sigma_c = f_{ct} \cdot \left(0.25 - 0.05 \cdot \frac{w}{w_1} \right) \text{ for } w_1 < w \leq w_c \quad (16b)$$

where $w_1 = G_F/f_{ct}$; $w_c = 5 \cdot G_F/f_{ct}$; and $G_F = 0.073 \cdot f_c^{0.18}$ = fracture energy of concrete in tension (f_c in MPa, G_F in N/mm).

As M_u is the moment at the yielding of steel in tension, the stress-strain relationship σ_s - ε_s of the rebar is modeled with the elastic-perfectly plastic constitutive law illustrated in Fig. 4(b) (fib 2012)

$$\sigma_s = E_s \cdot \varepsilon_s \text{ for } 0 \leq \varepsilon_s < \varepsilon_y = f_y/E_s \quad (17a)$$

$$\sigma_s = f_y \text{ for } \varepsilon_y = f_y/E_s \leq \varepsilon_s < \varepsilon_u \quad (17b)$$

where E_s , f_y and ε_u are the modulus of elasticity, the yielding strength, and the ultimate strain of steel rebar, respectively.

Finally, the following bond-slip relationship τ - s , proposed by Model Code 2010 (Fib 2012) and depicted in Fig. 5(b), is used

where $\tau_{\max} = 2.5 \cdot f_c^{0.5}$ (f_c in MPa); $\tau_f = 0.4 \cdot \tau_{\max}$ $\alpha = 0.4$; $s_1 = 1.0$ mm; $s_2 = 2.0$ mm; and $s_3 = c_{\text{clear}}$ = clear distance between the ribs of the rebar (in mm). To take into account the possibility of

$$\tau = \tau_{\max} \cdot \left(\frac{s}{s_1} \right)^\alpha \text{ for } 0 \leq s < s_1 \quad (18a)$$

$$\tau = \tau_{\max} \quad \text{for } s_1 \leq s < s_2 \tag{18b}$$

$$\tau = \tau_{\max} - (\tau_{\max} - \tau_f) \cdot \frac{s - s_2}{s_3 - s_2} \quad \text{for } s_2 \leq s < s_3 \tag{18c}$$

$$\tau = \tau_f \quad \text{for } s_3 \leq s \tag{18d}$$

the splitting failure at the interface between rebar and concrete (Giuriani and Plizzari 1998), the reduced bond strength $\tau_{u,\text{split}}^2$ (Fib 2012) has been considered (see the dashed line represented in Fig.5(b))

2.3 Numerical solution of the problem

All the equations previously introduced define the so-called “tension-stiffening” problem, which has to be solved within the one-dimensional domain of length l_{tr} . This is possible by applying the iterative procedure illustrated in Fig. 6 and described by the following points (Fantilli, Ferretti *et al.* 1999, Fantilli and Chiaia 2013), in which the subscript i refers to the abscissa $0 \leq z_i \leq l_{tr}$:

1. Assign a value to \bar{w} in the cracked cross-section (see Fig.2 (a) and Fig.3 (a)).
2. Assume a trial value for crack depth h_w (where $c < h_w < H$ – Fig. 2(a) and Fig. 3(a)).
3. Assume a trial value for x (i.e., the distance from the top edge to the neutral axis in the cracked cross-section of Fig. 3(a)).
4. Assuming the linearity of both the strain and the crack profile, define the state of stress in the cracked cross-section (Fig. 3(a)) through Eqs. (13)-(17), and calculate the resultant N (Eq. (6)).
5. If $N \neq 0$, then change x and go back to step 4.
6. Compute the internal bending moment M in the cracked cross-section (Eq. (7)).
7. Calculate the slip s_0 in the cracked cross-section (where $z_i = 0$) (Eq. (10)).
8. Evaluate the state of strain ($\varepsilon_l = \varepsilon_s = \varepsilon_c$ – Eq. (3)) at the level of reinforcement in the Stage I cross-section (Fig.3(b)).

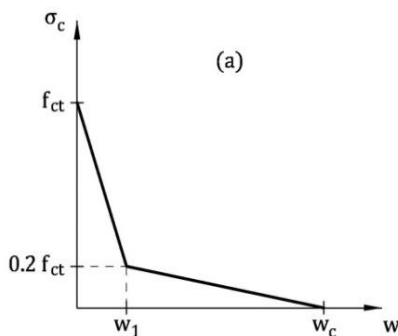


Fig. 5(a) Residual stress on the crack surface and bond stress at the interface of rebar and concrete in tension (Fib 2012): Stress-crack opening displacement relationship

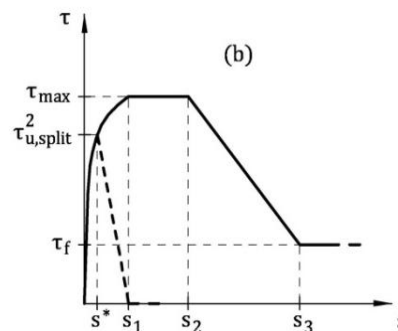


Fig. 5(b) Residual stress on the crack surface and bond stress at the interface of rebar and concrete in tension (Fib 2012): Bond-slip model

9. Consider Δl as a small part of the unknown $l_{tr} < L$ (= span of the beam), and define $z_i = i \cdot \Delta l$ (where $i = 1, 2, 3, \dots$).

10. For each i (or z_i) calculate:

- The bond stress τ_i , related to the slip s_{i-1} (Eq. (18)).
- The strain $\varepsilon_{s,i}$ in the reinforcement, by using Eq. (4) (and Eq. (17(a)) written in the finite difference form

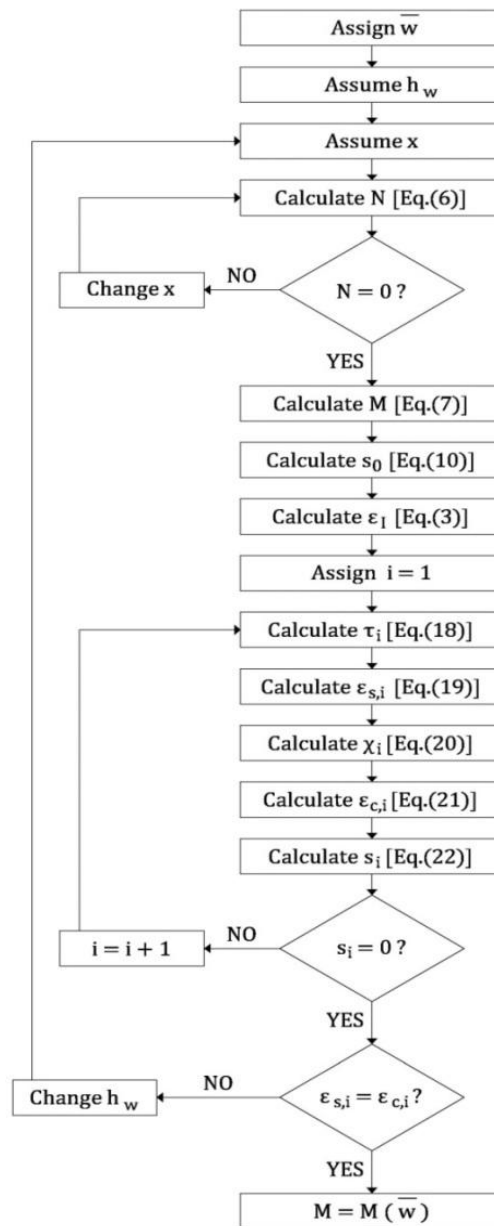


Fig. 6 Flow chart of the general model

$$\epsilon_{s,i} = \epsilon_{s,i-1} - \frac{4}{\phi \cdot E_s} \cdot \tau_i \cdot \Delta l \tag{19}$$

- The similarity coefficient χ_i (Eq. (8))

$$\chi_i = \frac{\epsilon_{s0} - \epsilon_{s,i}}{\epsilon_{s0} - \epsilon_1} \tag{20}$$

- The strain of concrete $\epsilon_{c,i}$ at the level of reinforcement (Eq.(9))

$$\epsilon_{c,i} = \epsilon_{c0} - \chi_i \cdot (\epsilon_{c0} - \epsilon_1) \tag{21}$$

- The slip s_i by means of the finite difference form of Eq. (5)

$$s_i = s_{i-1} - (\epsilon_{s,i} - \epsilon_{c,i}) \cdot \Delta l \tag{22}$$

11. When $s_i = 0$, if $\epsilon_{s,i} \neq \epsilon_{c,i}$, change h_w and go back to step 3.

For a given \bar{w} , such procedure calculates the corresponding internal moment M . Thus, by varying the assigned crack width, the complete $M-\bar{w}$ curve can be obtained. This curve starts from M_{cr} (elastically evaluated), which corresponds to $\bar{w}=0$.

3. Definition of the ductility index

The proposed procedure has been used to plot the $M-\bar{w}$ curves of 36 ideal LRC beams in three point bending (Fig. 7). They are divided into 12 groups of 3 beams, having the same geometrical and material properties, but with different amounts of reinforcement in tension. As illustrated in Fig. 7, the width B and the span L of the beams are 0.5 and 6 times the depth H , respectively. Compressive strength of concrete varies (i.e., $f_c = 30, 45$ and 60 MPa), whereas the same properties of steel (i.e., $f_y = 450$ MPa and $E_s = 210$ GPa) are assumed for rebar of diameter ϕ .

Table 1 summarizes the characteristics of all the beams, which are labelled with the acronym SX_CYY_φZ_W: X depends on the beam depth ($X = 1$ for 200 mm, and $X = 2$ for 400 mm); YY is the concrete strength (30 MPa, 45 MPa or 60 MPa); Z is the rebar diameter; and W is a number (1, 2, or 3) associated to the value of A_s .

As an example, the $M-\bar{w}$ curves of the beams S2_C30_φ8_1 and S2_C30_φ8_2 are reported in Fig. 8(a) and Fig. 8(b), respectively. Two stationary points, concerning the effective cracking moment (M_{cr*}) and the ultimate bending moment (M_u), are clearly evident in both the Figures.

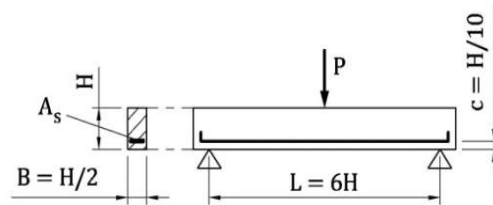


Fig. 7 Ideal LRC beams in three point bending

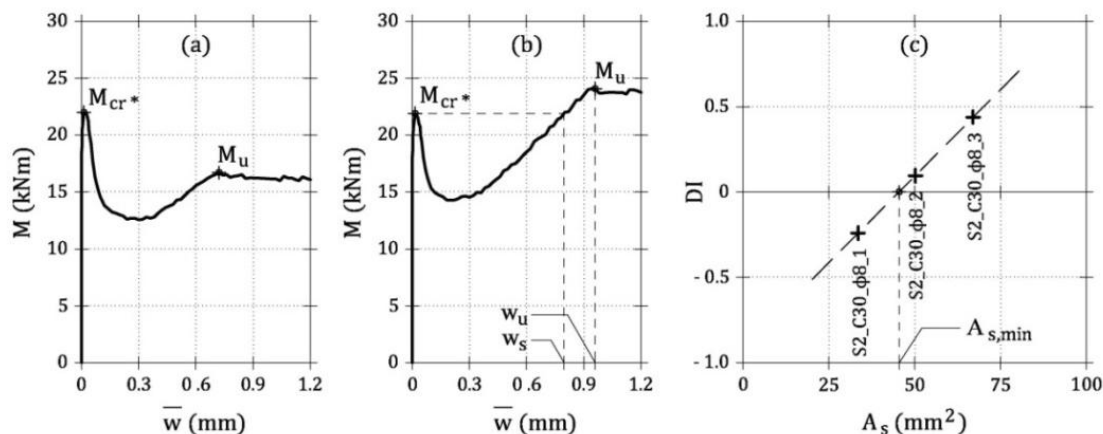


Fig. 8 Application of the general model to the beams of group 3 (see Table 1 and Table 2): (a) $M-\bar{w}$ curve of S2_C30_φ8_1 beam; (b) $M-\bar{w}$ curve of S2_C30_φ8_2 beam and definition of w_s and w_u ; (c) $DI-A_s$ relationship and definition of $A_{s,min}$

Fig. 8(a) shows the response of an under-reinforced concrete beam (with $M_u < M_{cr^*}$), whereas the $M-\bar{w}$ curve illustrated in Fig. 8(b) (with $M_u > M_{cr^*}$) represents the typical behavior of a beam reinforced with $A_s > A_{s,min}$. The values of M_{cr^*} and M_u , taken on the $M-\bar{w}$ curves of the 36 ideal LRC beams, are collected in Table 2.

The ductile behavior of LRC beams, as stated by Eq. (1), corresponds to a positive value of the following ductility index (DI)

$$DI = \frac{M_u - M_{cr^*}}{M_{cr^*}} = \frac{P_u - P_{cr^*}}{P_{cr^*}} \quad (23)$$

As under-reinforced concrete beams exhibit $DI < 0$, the minimum reinforcement for the required ductility can be computed by imposing $DI = 0$.

Table 2 reports the values of DI calculated for the ideal beams investigated herein. For each group of beams (e.g., those of group 3 in Fig. 8(c)), a linear relationship between DI and A_s is attained. In other words, referring to Eq. (23), if M_{cr^*} is assumed to be independent of the quantity of rebar, the well-known linear increment of M_u with A_s can be recognized in Fig. 8(c). Thus, the values of $A_{s,min}$, detected for each group with the intersection between the line $DI-A_s$ and the horizontal axis (i.e., $DI = 0$), are reported in Table 2. Although beams with different geometrical properties have been analyzed, the procedure for computing $A_{s,min}$ is the same and, therefore, it is capable of capturing the size effect.

If the normalized reinforcement ratio $a = A_s/A_{s,min}$ is introduced (Fig. 9(a)), the existence of a linear function $DI-a$ can be argued. This line certainly passes through the point representing a beam reinforced with $A_{s,min}$ (i.e., $a=1$ and $DI=0$). Moreover, the definition of DI suggests another point of the line, which corresponds to an unreinforced concrete beam (i.e., $a=0$). In such a case, $M_u=0$ can be assumed and, according to Eq. (23), $DI=-1$. As a result, a single and unitary slope can be deduced for the linear relationship proposed herein. This is substantially confirmed by the least square approximation of all the $DI-a$ couples previously computed for the 36 ideal LRC

Table 1 Properties of the ideal LRC beams

Group	Beam	B (mm)	H (mm)	L (mm)	(mm)	f_c (MPa)	A_s (mm ²)
1	S1_C30_φ4_1	100	200	1200	4	30	25
	S1_C30_φ4_2						38
	S1_C30_φ4_3						50
2	S1_C30_φ5_1	100	200	1200	5	30	20
	S1_C30_φ5_2						39
	S1_C30_φ5_3						59
3	S2_C30_φ8_1	200	400	2400	8	30	101
	S2_C30_φ8_2						151
	S2_C30_φ8_3						201
4	S2_C30_φ10_1	200	400	2400	10	30	79
	S2_C30_φ10_2						157
	S2_C30_φ10_3						236
5	S1_C45_φ5_1	100	200	1200	5	45	39
	S1_C45_φ5_2						59
	S1_C45_φ5_3						79
6	S1_C45_φ6_1	100	200	1200	6	45	28
	S1_C45_φ6_2						57
	S1_C45_φ6_3						85
7	S2_C45_φ8_1	200	400	2400	8	45	101
	S2_C45_φ8_2						201
	S2_C45_φ8_3						302
8	S2_C45_φ10_1	200	400	2400	10	45	157
	S2_C45_φ10_2						236
	S2_C45_φ10_3						314
9	S1_C60_φ5_1	100	200	1200	5	60	39
	S1_C60_φ5_2						59
	S1_C60_φ5_3						79
10	S1_C60_φ6_1	100	200	1200	6	60	28
	S1_C60_φ6_2						57
	S1_C60_φ6_3						85
11	S2_C60_φ8_1	200	400	2400	8	60	201
	S2_C60_φ8_2						251
	S2_C60_φ8_3						302
12	S2_C60_φ10_1	200	400	2400	10	60	157
	S2_C60_φ10_2						236
	S2_C60_φ10_3						314

Table 2 Evaluation of the ductility index, of the minimum reinforcement and of the crack width in the ideal LRC beams

Group	Beam	M_{cr}^* (kNm)	M_u (kNm)	DI	$A_{s,min}$ (mm ²)	a	w_s (mm)	w_u (mm)	$w_{s,EC2}$ (mm)
1	S1_C30_φ4_1	2.95	2.23	-0.24		0.70	/	0.42	/
	S1_C30_φ4_2	2.94	3.06	0.04	36	1.06	0.50	0.56	0.37
	S1_C30_φ4_3	2.94	3.97	0.35		1.41	0.38	0.68	0.27
2	S1_C30_φ5_1	3.03	1.98	-0.35		0.55	/	0.28	/
	S1_C30_φ5_2	3.00	3.18	0.06	36	1.10	0.42	0.48	0.37
	S1_C30_φ5_3	3.03	4.57	0.51		1.64	0.26	0.64	0.24
3	S2_C30_φ8_1	21.99	16.70	-0.24		0.74	/	0.72	/
	S2_C30_φ8_2	21.88	23.97	0.10	136	1.11	0.78	0.92	0.68
	S2_C30_φ8_3	21.77	31.31	0.44		1.47	0.60	1.14	0.50
4	S2_C30_φ10_1	22.67	13.69	-0.40		0.56	/	0.48	/
	S2_C30_φ10_2	22.37	25.10	0.12	140	1.13	0.68	0.82	0.67
	S2_C30_φ10_3	22.44	36.16	0.61		1.69	0.48	1.06	0.44
5	S1_C45_φ5_1	3.92	3.27	-0.17		0.81	/	0.42	/
	S1_C45_φ5_2	3.93	4.63	0.18	49	1.21	0.40	0.56	0.31
	S1_C45_φ5_3	3.93	6.07	0.54		1.62	0.32	0.70	0.23
6	S1_C45_φ6_1	4.03	2.63	-0.35		0.58	/	0.30	/
	S1_C45_φ6_2	3.99	4.52	0.13	48	1.17	0.38	0.48	0.33
	S1_C45_φ6_3	4.01	6.57	0.64		1.75	0.24	0.64	0.21
7	S2_C45_φ8_1	29.18	16.97	-0.42		0.55	/	0.60	/
	S2_C45_φ8_2	28.41	31.31	0.10	181	1.11	0.82	0.96	0.64
	S2_C45_φ8_3	28.23	45.87	0.63		1.66	0.58	1.40	0.41
8	S2_C45_φ10_1	29.10	25.48	-0.12		0.87	/	0.70	/
	S2_C45_φ10_2	29.00	36.77	0.27	182	1.30	0.62	0.94	0.55
	S2_C45_φ10_3	28.91	48.32	0.67		1.73	0.50	1.18	0.40
9	S1_C60_φ5_1	4.69	3.34	-0.29		0.68	/	0.38	/
	S1_C60_φ5_2	4.65	4.70	0.01	58	1.02	0.48	0.52	0.36
	S1_C60_φ5_3	4.64	6.13	0.32		1.36	0.38	0.62	0.26
10	S1_C60_φ6_1	4.83	2.70	-0.44		0.49	/	0.28	/
	S1_C60_φ6_2	4.76	4.58	-0.04	58	0.98	/	0.44	/
	S1_C60_φ6_3	4.75	6.66	0.40		1.46	0.32	0.58	0.25
11	S2_C60_φ8_1	34.03	31.97	-0.06		0.93	/	0.88	/
	S2_C60_φ8_2	33.78	39.06	0.16	215	1.17	0.80	1.02	0.59
	S2_C60_φ8_3	33.87	46.79	0.38		1.40	0.70	1.30	0.49
12	S2_C60_φ10_1	35.25	25.77	-0.27		0.73	/	0.64	/
	S2_C60_φ10_2	34.40	37.40	0.09	218	1.10	0.74	0.86	0.65
	S2_C60_φ10_3	34.55	48.82	0.41		1.46	0.58	1.04	0.48

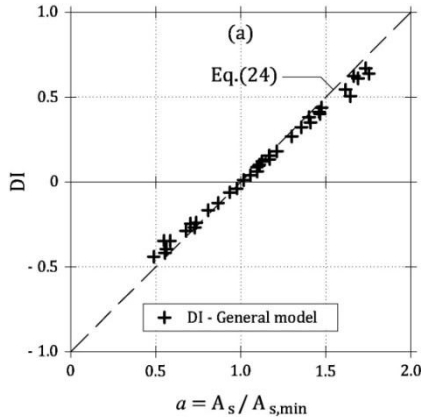


Fig. 9(a) The proposed linear relationships in comparison with the results of the general model: DI vs. a (Eq. (24))

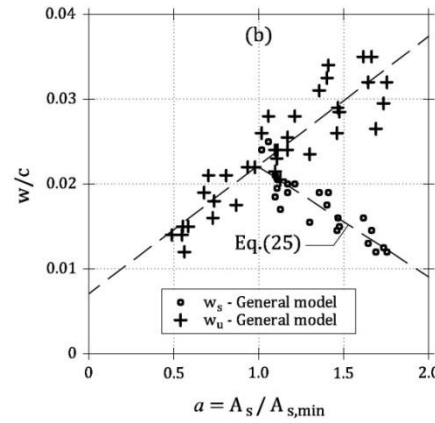


Fig. 9(b) The proposed linear relationships in comparison with the results of the general model: w/c vs. a (Eq. (25))

beams (Fig. 9(a)). In other words, by means of the following equation, the ductility index, previously introduced for a single group of beams, can be generally applied to all the LRC beams regardless of the size and of the material properties (Fig. 9(a))

$$DI = a - 1 \tag{24}$$

3.1 Control of cracking

In addition to the static requirement of Eq. (1), the minimum reinforcement must also guarantee cracking control in the serviceability state (Levi 1985). Hence, the conventional crack width in service, w_s , can be defined on the hardening branch of the $M - \bar{w}$ curves when $M = M_{cr*}$ (Fig. 8(b)). Obviously, this value can only be computed in the case of a ductile response of the LRC beams (i.e., $M_u > M_{cr*}$). On the other hand, at the ultimate condition (i.e. $M = M_u$) the corresponding crack width is w_u (Fig. 8(b)).

Similarly to the case of DI in Fig. 9(a), w_s and w_u need to be normalized. As the two variables that mainly affect crack width are the diameter ϕ of rebar and concrete cover c (Beeby 2004, Beeby 2005), these values can be divided by the factor $\phi^\gamma \cdot c^{1-\gamma}$, where the exponent γ varies between 0 and 1. Assuming a linear regression, the total square deviations of w_s and w_u , both computed with the general model, are minimum when $\gamma = 0$. In other words, concrete cover appears as the most important parameter governing crack width (Beeby 2004).

Hence, a general relationship between the normalized service crack width and a can be represented by the following equation (see Fig. 9(b))

$$\frac{w_s}{c} = \psi \cdot a + \omega \tag{25}$$

where $\psi = -0.013$ and $\omega = 0.035$.

As shown in Fig. 9(b), for a given value of concrete cover, w_s decreases with a , and contemporarily w_u increases. Thus, to reduce crack width in the serviceability stage (i.e., w_s), the total area of rebar needs to be increased.

4. Experimental results compared with the predictions of DI

To further verify the accuracy of the proposed linear relationship, the predicted values of DI (i.e., Eq. (24)) are compared with those measured in 32 LRC beams tested in different experimental campaigns (Bosco, Carpinteri *et al.* 1990, Brincker, Henriksen *et al.* 1999, Carpinteri 1989, Carpinteri, Ferro *et al.* 1999, Elrakib 2013, Lange-Kornbak and Karihaloo 1999, Ruiz, Elices *et al.* 1999). Specifically, 14 homogeneous groups of at least two beams in bending, which unequivocally fail in tension (having the same geometrical and material properties, but different amounts of reinforcement), are taken into consideration. As shown by Table 3, where the main properties of the 32 beams (labelled with the original names given by the Authors) are reported, a wide range of geometrical sizes and material strengths are investigated. A certain variation of f_y within groups of homogenous beams is tolerated, especially for the rebar which do not show a well-defined yielding stress.

In such situation, as illustrated in Fig. 8(c), $A_{s,min}$ can be evaluated when the values of DI are known from the tests, generally performed on three point bending beams, with the exception of the four point bending tests by Elrakib (2013). The experimental values of P_{cr*} and P_u , and of DI (Eq. (23)) as well, are included in Table 4. In the same Table, the minimum reinforcement area, computed for each homogeneous group of LRC beams (Fig. 8(c)), and the corresponding values of $a = A_s/A_{s,min}$ are also collected.

Both the points $[DI, a]$ experimentally measured, and the proposed linear function (i.e., Eq. (24)), are depicted in the diagram of Fig. 10(a). In spite of the dispersion of the results, the tests confirm the linear dependence of DI and a , as stated by Eq. (24), especially when $DI \neq 0$. Conversely to the direct calculation methods, the proposed procedure for the evaluation of $A_{s,min}$,

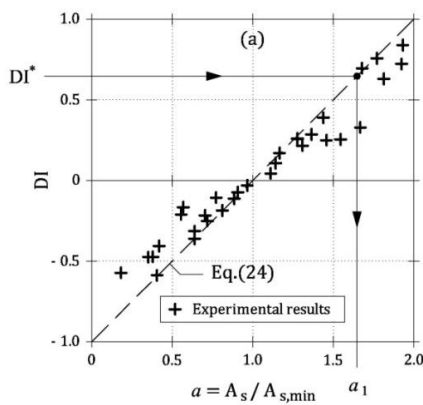


Fig. 10(a) The results of the proposed linear relationships compared with: the experimental data of DI

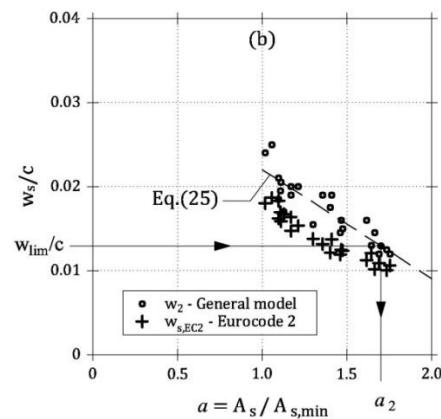


Fig. 10(b) The results of the proposed linear relationships compared with: the values of w_s computed in accordance with Eurocode 2 (CEN 2004)

Table 3 Properties of LRC beams tested in different experimental campaigns

Group	Beam	B (mm)	H (mm)	d (mm)	L (mm)	f_c (MPa)	f_y (MPa)	A_s (mm ²)	References	
I	A_1	150	100	90	600	75.7	637	13	(Bosco, Carpinteri <i>et al.</i> 1990)	
	A_2						569	39		
II	B_1	150	200	180	1200	75.7	569	20		
	B_2						569	59		
III	C_1	150	400	360	2400	75.7	637	25		
	C_2						569	79		
	C_3						441	201		
IV	HSC_0.14	100	100	90	1200	98.5	740	13		(Brincker, Henriksen <i>et al.</i> 1999)
	HSC_0.25						740	25		
V	B_1	150	200	180	1200	24.4	489	28		(Carpinteri 1989)
	B_2						489	57		
VI	D_1	200	800	720	4800	24.4	456	79		
	D_2						456	157		
	D_3						456	236		
VII	A012-06	100	100	90	600	40.0	604	20	(Carpinteri, Ferro <i>et al.</i> 1999)	
	A025-06						604	39		
VIII	A012-12	100	100	90	1200	40.0	604	20		
	A025-12						604	39		
IX	B501	250	400	361	3300	43.2	480	157	(Elrakib 2013)	
	B502						515	226		
X	B751	250	400	361	3300	60.6	495	192		
	B752						501	270		
XI	A_012_06#1	100	100	80	600	43.0	485	13	(Lange-Kornbak and Karihaloo 1999)	
	A_012_06#3							13		
	A_025_06#1							25		
	A_025_06#3							25		
XII	D1-R2X	50	75	64	300	39.5	538	5	(Ruiz, Elices <i>et al.</i> 1999)	
	D1-R3X						538	10		
XIII	D2-R1X	50	150	128	600	39.5	538	5		
	D2-R2X						538	10		
XIV	D3-R1X	50	300	255	1200	39.5	538	10		
	D3-R2X						538	20		

based on the measure of the ductility index and not affected by size effect, is generally valid. Indeed, if the non-dimensional parameters DI and a are introduced, the simplified hypotheses used in the general model (i.e., the linear crack profile, the cohesive and the bond-slip models, the

Table 4 Evaluation of the ductility index and of the minimum reinforcement in LRC beams tested in different experimental campaigns

Group	Beam	P_{cr}^* (kN)	P_u (kN)	DI	$A_{s,min}$ (mm ²)	a	References	
I	A_1	11.8	7.0	-0.41	30	0.42	(Bosco, Carpinteri <i>et al.</i> 1990)	
	A_2	12.5	15.2	0.22		1.31		
II	B_1	19.6	10.3	-0.47	52	0.38		
	B_2	20.9	23.1	0.11		1.14		
III	C_1	36.7	15.7	-0.57	138	0.18		
	C_2	38.8	32.4	-0.17		0.57		
	C_3	43.2	54.0	0.25		1.46		
IV	HSC_0.14	3.5	3.2	-0.07	14	0.91		(Brincker, Henriksen <i>et al.</i> 1999)
	HSC_0.25	3.6	5.9	0.63		1.81		
V	B_1	11.3	10.1	-0.11	37	0.77		(Carpinteri 1989)
	B_2	14.1	17.7	0.26		1.55		
VI	D_1	35.2	27.8	-0.21	141	0.56		
	D_2	43.4	45.3	0.04		1.11		
	D_3	45.6	60.6	0.33		1.67		
VII	A012-06	7.1	6.3	-0.11	22	0.89	(Carpinteri, Ferro <i>et al.</i> 1999)	
	A025-06	7.0	12.3	0.76		1.77		
VIII	A012-12	3.2	3.1	-0.03	20	0.97		
	A025-12	3.1	5.7	0.84		1.93		
IX	B501	37.6	44.0	0.17	135	1.17	(Elrakib 2013)	
	B502	44.5	75.5	0.70		1.68		
X	B751	39.3	50.5	0.28	140	1.36		
	B752	46.1	79.4	0.72		1.92		
XI	A_012_06#1	6.9	4.4	-0.36	20	0.64	(Lange-Kornbak and Karihaloo 1999)	
	A_012_06#3	7.0	4.8	-0.31				
	A_025_06#1	7.0	8.8	0.26				
	A_025_06#3	7.3	9.2	0.26				
XII	D1-R2X	3.6	2.7	-0.25	7	0.72	(Ruiz, Elices <i>et al.</i> 1999)	
	D1-R3X	3.6	5.0	0.39		1.44		
XIII	D2-R1X	6.8	2.8	-0.59	12	0.41		
	D2-R2X	6.5	5.3	-0.19		0.81		
XIV	D3-R1X	11.3	5.9	-0.48	28	0.35		
	D3-R2X	11.3	8.9	-0.22		0.70		

constitutive law of steel rebar, the constant bending moment inside l_{tr}) seem to be irrelevant to assess the brittle/ductile behavior of LRC beams. In other words, they affect in the same manner

both the values of P_{cr*} and P_u in Eq. (23), and, despite the nonlinearities, a linear DI - a function is obtained and confirmed by several tests.

As a consequence, a simple-to-apply procedure, requiring the use of Eq. (24) and the results of tests on a single full-scale beam, can provide the minimum reinforcement for static reasons. Indeed, from the ductility index measured in the tests (i.e., DI^* in Fig. 10(a)), the corresponding value of the normalized reinforcement ratio a_1 can be obtained through Eq. (24) (or graphically in Fig. 10(a)). Then the calculation of the minimum reinforcement for ultimate conditions is possible (i.e., $A_{s,min}=A_s/a_1$, where A_s is the reinforcement of the tested beam).

4.1 Control of cracking

The available tests devoted to the evaluation of the minimum reinforcement area do not report, in general, any data regarding crack width. Therefore, the values of w_s computed for the ideal LRC beams by means of Eq. (25) are compared with those of Eurocode 2 formula (CEN 2004)

$$w_{s,EC2} = s_{r,max} \cdot (\varepsilon_{sm} - \varepsilon_{cm}) \quad (26)$$

In Eq. (26), crack spacing $s_{r,max}$ is related to the conditions of widely spaced rebar (because of the weak reinforcement present in LRC beams), and the strain difference $(\varepsilon_{sm}-\varepsilon_{cm})$ refers to the stress level produced by M_{cr*} .

The values of $w_{s,EC2}$ computed for the ideal beams are collected in Table 2, and the points $[w_{s,EC2}/c, a]$ are reported in the non-dimensional diagram of Fig. 10(b). In the latter, crack width calculated with the general model and Eq. (25) are also depicted. The values are dispersed within this non-dimensional chart, even if Eq. (25) appears as the upper bound approximation of Eurocode 2 predictions, which seems not to consider the size effect on crack width (Yasir Alam, Lenormand, *et al.* 2010).

Accordingly, Eq. (25) can be used as an additional design relationship to determine the minimum reinforcement for controlling crack width. When the normalized maximum crack width is established (i.e., w_{lim}/c in Fig. 10(b)), it is possible to obtain the normalized reinforcement ratio $a_2=(w_{lim}/c-\omega)/\psi$. Then, if $a_2 < 1$, $A_{s,min}$ computed with Eq. (24) is also sufficient to guarantee $w < w_{lim}$. On the other hand, in the case $a_2 > 1$, $A_{s,min}$ needs to be increased by means of the multiplying factor a_2 obtained from Eq. (25). Indeed, an increment of the minimum reinforcement should be provided to reduce crack width in service.

For the 14 groups of LRC beams previously considered, whose properties are reported in Table 3 and Table 4, the minimum reinforcement $A_{s,min}^{(i)}$ is determined with Eqs. (24)-(25) for two values of w_{lim} (i.e., 0.6 and 0.3 mm). For the same beams, the formulae of ACI 318-14 (ACI 2014) and Model Code 2010 (Fib 2012) are also applied, and all the values are reported in Table 5.

In some cases (e.g., the beams of group I in Fig. 11(a)), the increment of the minimum reinforcement area is not necessary. This is true not only for $w_{lim}=0.6$ mm but also for $w_{lim}=0.3$ mm, which is the limit value suggested by Eurocode 2 (CEN 2004) for the most aggressive exposure classes. Such a reinforcement is nearly coincident with that computed with Model Code 2010 (Fib 2012), but it is lower than that suggested by ACI 318-14 (ACI 2014). In fact, the latter often over-estimates the minimum reinforcement (Said and Elrakib 2013). However, in other cases (e.g., the beams of group XIV), with respect to the minimum reinforcements computed with the two building codes (ACI 2014, Fib 2012), an increment of steel rebar is necessary to maintain crack width lower than $w_{lim} = 0.3$ mm (see Table 5 and Fig. 11(b)).

Conversely to rigorous methods, based on the results of the material characterization tests (see

Table 5 Minimum reinforcement calculated in accordance with the proposed model, ACI 318-14 (ACI 2014), and Model Code 2010 (Fib 2012), for some LRC beams tested in different experimental campaigns

Group	$A_{s,min}^{(l)}$ (mm ²)				References
	Eqs. (24)-(25) $w_{lim} = 0.6$ mm	Eqs. (24)-(25) $w_{lim} = 0.3$ mm	ACI 318-14 (ACI 2014)	MC2010 (Fib 2012)	
I	27	27	49	27	(Bosco, Carpinteri <i>et al.</i> 1990)
II	45	70	103	56	
III	161	222	218	119	
IV	14	14	30	16	(Brincker, Henriksen <i>et al.</i> 1999)
V	38	59	76	28	(Carpinteri 1989)
VI	302	343	435	159	
VII	22	22	23	12	(Carpinteri, Ferro <i>et al.</i> 1999)
VIII	21	21	23	12	
IX	202	281	297	152	(Elrakib 2013)
X	231	322	352	195	
XI	19	30	27	14	(Lange-Kornbak and Karihaloo 1999)
XII	7	7	9	5	(Ruiz, Elices <i>et al.</i> 1999)
XIII	12	20	19	9	
XIV	37	48	37	18	

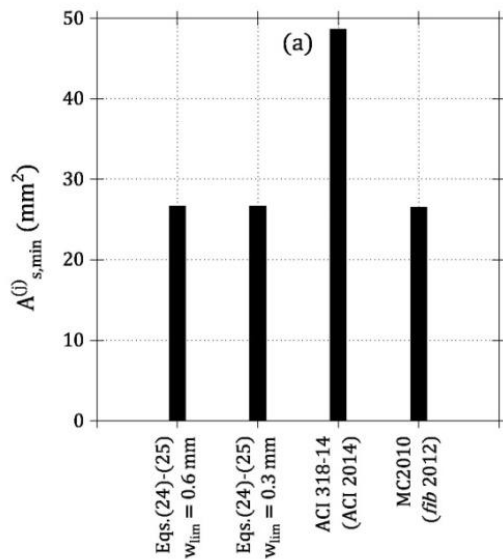


Fig. 11(a) The minimum reinforcement calculated in accordance with the proposed model, ACI 318-14 (ACI 2014), and Model Code 2010 (Fib 2012): The beams of group I (see Table 5)

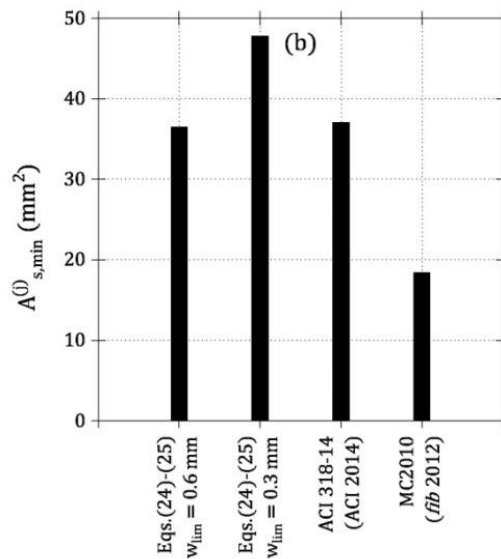


Fig. 11(b) The minimum reinforcement calculated in accordance with the proposed model, ACI 318-14 (ACI 2014), and Model Code 2010 (Fib 2012): The beams of group XIV (see Table 5)

for instance Carpinteri (Ed) 1999), the models proposed herein (i.e., Eqs. (24)-(25)) only require few full-scale beam tests to calculate $A_{s,min}$. Such approach has been successfully applied to evaluate the minimum reinforcement of the precast plates of a bridge (Fantilli, Cavallo *et al.* 2015).

5. Conclusions

According to the analyses previously described, the following conclusions can be drawn

- When the ultimate bending moment equates the effective cracking moment, which is the condition for computing the minimum reinforcement for static reasons ($A_{s,min}$) in LRC beams, the ductility index DI , given by Eq. (23), is equal to zero.

- The numerical results of a general model, and the data measured in several experimental analyses, show that the values of DI linearly increase with the normalized reinforcement ratio $a=A_s/A_{s,min}$ (Eq.(24)), regardless of the beam size and of the material properties.

- A further linear relationship between the normalized service crack width w_s/c and the ratio a can also be obtained from the general model (Eq. (25)). This relationship is the upper bound approximation of crack widths, if estimated in accordance with Eurocode 2 (CEN 2004).

- With respect to the current approaches, Eqs. (24)-(25), accompanied by tests on a single full-scale LRC beam in bending, define a rigorous but practical tool for the evaluation of the minimum reinforcement. As the design-by-testing procedure can be adapted to different limits of crack width, it can be used to satisfy both the ultimate and the serviceability limit states.

Finally, further studies should be devoted to hybrid structures, in order to extend the present approach to LRC beams reinforced with fibers and steel rebar.

Acknowledgments

The grant given by the Italian Laboratories University Network of seismic engineering (ReLUIS), and used to develop this research work, is gratefully acknowledged.

References

- ACI (2014), *ACI 318-14: Building Code Requirements for Structural Concrete and Commentary*, American Concrete Institute, Farmington Hills, Michigan, USA.
- Bažant, Z.P. and Cedolin, L. (1991), *Stability of Structures: Elastic, Inelastic, Fracture and Damage Theories*, Oxford University Press, New York, U.S.A.
- Beeby, A.W. (2004), "The influence of the parameter ϕ/ρ_{eff} on crack widths", *Struct. Concrete.*, **5**(2), 71-83.
- Beeby, A.W. (2005), "Discussion-the influence of the parameter ϕ/ρ_{eff} on crack widths", *Struct. Concrete*, **6**(4), 155-165.
- Borosnyói, A. and Balázs, G.L. (2005), "Models for flexural cracking in concrete: the state of the art", *Struct. Concrete*, **6**(2), 53-62.
- Bosco, C., Carpinteri, A. and Debernardi, P.G. (1990), "Minimum reinforcement in high-strength concrete", *J. Struct. Eng.*, **116**(2), 427-437.
- Brincker, R., Henriksen, M.S., Christensen, F.A. and Heshe, G. (1999), "Size effects on the bending

- behaviour of reinforced concrete beams”, *Eur. Struct. Integr. Soc.*, **24**, 127-180.
- Carpinteri, A. (1989), “Minimum reinforcement in reinforced concrete beams”, *RILEM TC 90-FMA, Code Work*, Cardiff, September.
- Carpinteri, A. (1999), *Minimum Reinforcement in Concrete Members*, Elsevier, Oxford, U.K.
- Carpinteri, A., Cadamuro, E. and Corrado, M. (2014), “Minimum flexural reinforcement in rectangular and T-section concrete beams”, *Struct. Concrete*, **15**(3), 361-372.
- Carpinteri, A., Ferro, G., Bosco, C. and Elkatieb, M. (1999), “Scale effects and transitional failure phenomena of reinforced concrete beams in flexure”, *Eur. Struct. Integr. Soc.*, **24**, 1-30.
- CEB (1998), *CEB Bulletin 242: Ductility of Reinforced Concrete Structures*, European Committee for Concrete, Lausanne, Switzerland.
- CEN. (2004), *EN 1992-1-1: Eurocode 2: Design of Concrete Structures - Part 1-1: General Rules and Rules for Buildings*, European Committee for Standardization, Brussels, Belgium.
- Elrakib, T.M. (2013), “Performance evaluation of HSC beams with low flexural reinforcement”, *HBRC J.*, **9**(1), 49-59.
- Fantilli, A.P. and Chiaia, B. (2013), “Golden ratio in the crack pattern of reinforced concrete structures”, *J. Eng. Mech.*, **139**(9), 1178-1184.
- Fantilli, A.P., Cavallo, A.D. and Pistone, G. (2015), “Fiber-reinforced lightweight concrete slabs for the maintenance of the Soleri Viaduct”, *Eng. Struct.*, **99**, 184-191.
- Fantilli, A.P., Ferretti, D. and Rosati, G. (2005), “Effect of bar diameter on the behavior of lightly reinforced concrete beams”, *ASCE J. Mater. Civ. Eng.*, **17**(1), 10-18.
- Fantilli, A.P., Ferretti, D., Iori, I. and Vallini, P. (1999), “Behaviour of R/C elements in bending and tension: The problem of minimum reinforcement ratio”, *Eur. Struct. Integr. Soc.*, **24**, 99-125.
- Fib (2000), *Fib Bulletin 10: Bond of Reinforcement in Concrete*, International Federation for Structural Concrete, Lausanne, Switzerland.
- Fib (2012), *Fib Bulletin 65-66: Model Code 2010-Final Draft*, International Federation for Structural Concrete, Lausanne, Switzerland.
- Giuriani, E. and Plizzari, G.A. (1998), “Interrelation of splitting and flexural cracks in RC beams”, *J. Struct. Eng.*, **124**(9), 1032-1040.
- Lange-Kornbak, D. and Karihaloo, B.L. (1999), “Fracture mechanical prediction of transitional failure and strength of singly-reinforced beams”, *Eur. Struct. Integr. Soc.*, **24**, 31-66.
- Levi, F. (1985), “On minimum reinforcement in concrete structures”, *J. Struct. Eng.*, **111**(12), 2791-2796.
- Maldague, J.C. (1965), “Établissement des lois moments-courbures”, *Annales de l'Institut Technique du Batiment et des Travaux Publics*, **213**, 1170-1218.
- Rizk, E. and Marzouk, H. (2011), “Experimental validation of minimum flexural reinforcement for thick HSC plates”, *ACI Struct. J.*, **108**(3), 332-340.
- Ruiz, G., Elices, M. and Planas, J. (1999), “Size effect and bond-slip dependence of lightly reinforced concrete beams”, *Eur. Struct. Integr. Soc.*, **24**, 67-97.
- Said, M. and Elrakib, T.M. (2013), “Experimental verification of the minimum flexural reinforcement formulas for HSC beams”, *IJCIET*, **4**(5), 152-167.
- Seguirant, S.J., Brice, R. and Khaleghi, B. (2010), “Making sense of minimum flexural reinforcement requirements for reinforced concrete members”, *PCI J.*, **55**(3), 64-85.
- Yasir Alam, S., Lenormand, T., Loukili, A. and Regoin, J.P. (2010), “Measuring crack width and spacing in reinforced concrete members”, *Proceedings of the 7th International conference on Fracture Mechanics of Concrete and Concrete Structures (FraMCoS-7)*, 377-382.